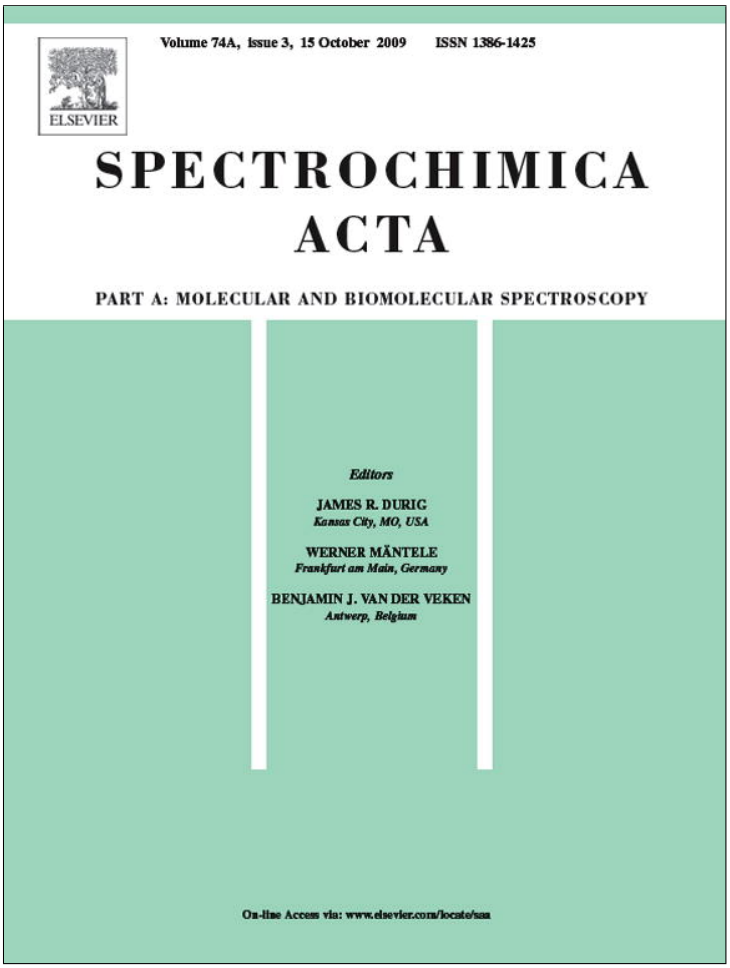

Spectrochimica Acta Part A 74 (2009) 635–641

Contents lists available at ScienceDirect

Spectrochimica Acta Part A: Molecular and Biomolecular Spectroscopy

journal homepage: www.elsevier.com/locate/saa

Biological potential study of metal complexes of sulphonylurea glibenclamide on the house fly, *Musca domestica* (Diptera—Muscidae): Preparation, spectroscopic and thermal characterization

Gehad G. Mohamed[a,*], S.M. Abdallah[b], M.A. Zayed[a], M.M.I. Nassar[c]

[a] *Chemistry Department, Faculty of Science, Cairo University, Giza, Egypt*
[b] *Workers University, Aswan, Egypt*
[c] *Insecticide Department, Faculty of Science, Cairo University, Giza, Egypt*

ARTICLE INFO

Article history:
Received 7 March 2009
Accepted 8 July 2009

Keywords:
Glibenclamide
Metal complexes
Spectroscopy
Molar conductance
Magnetic moment
Thermal analysis
Biological activity

ABSTRACT

The ligatation behaviour of sulphonylurea glibenclamide drug is studied in order to give an idea about its potentiality towards some transition metals in vitro systems. Metal complexes of glibenclamide (GCA; H_3L) drug are prepared and characterized based on elemental analyses, IR, diffused reflectance, magnetic moment, molar conductance and thermal analysis (TG and DTG) techniques. From the elemental analyses data, the complexes are proposed to have the general formulae $[M(H_3L)Cl_n(H_2O)_m]\cdot yH_2O$ (where M = Cr(III) ($n=3$, $m=1$, $y=3$); Mn(II) ($n=2$, $m=0$, $y=1$); Fe(III) ($n=3$, $m=1$, $y=0$), Co(II) ($n=2$, $m=2$, $y=0$); Ni(II) ($n=2$, $m=2$, $y=3$); Cu(II) ($n=2$, $m=2$, $y=2$) and Zn(II) ($n=2$, $m=0$, $y=0$). The molar conductance data reveal that all the metal chelates are non-electrolytes. IR spectra show that GCA is coordinated to the metal ions in a neutral bidentate manner with OO donor sites of the amide-*O* and sulphone-*O*. From the magnetic and solid reflectance spectra, it is found that the geometrical structures of these complexes are octahedral except Mn(II) and Zn(II) complexes which have tetrahedral structure. The thermal behaviour of these chelates is studied using thermogravimetric analysis (TG and DTG) technique. The activation thermodynamic parameters are calculated using Coats–Redfern method. The GCA drug, in comparison to its metal complexes also is screened for its biological activity against house fly, *Musca domestica* (Diptera—Muscidae). Dose of 5 μg/insect of GCA is topically applied against 3 days old larval instar of *M. domestica*. Survival of pupal and adult stages has been affected by the complexes of GCA more than larval instars. Morphogenic abnormalities of larvae, pupae and adults are studied. On the other hand pupation and adult emergence program is deteriorated by the effect of different chemicals.

1. Introduction

Currently the most commonly prescribed medications for Type 2 diabetes are metformin and the second generation sulfonylureas which include glipizide, gliclazide, glibenclamide and glimperide. For many patients with Type 2 diabetes, monotherapy with an oral antidiabetic agent is not sufficient to reach target glycaemic goals and multiple drugs may be necessary to achieve adequate control [1]. In such cases a combination of metformin and one of the sulfonylureas (SU) is used [2]. This combination can be achieved by taking each of the drugs separately or alternatively fixed formulations have been developed. Combinations of metformin and glipizide or gliclazide or glibenclamide are available commercially as single tablets. A combination tablet formulation is beneficial in terms of its convenience and patient compliance.

The measurement of the plasma concentrations of antidiabetic medications is important for studying the pharmacokinetics of these drugs, for adherence and drug monitoring in diabetic patients and for diagnostic purposes in factitious hypoglycaemia. The choice of treatment for diabetic patients is mainly dependent on the doctors' choice which should be dependent on the patients' clinical characteristics and the pharmacological properties of the various agents available, thus, for certain diabetic populations we can find patients who are prescribed glipizide, gliclazide, glimperide, glibenclamide, metformin or a combination of metformin and one of the sulfonylureas. Therefore, therapeutic monitoring requires the availability of a single method that can be used for all these possibilities in order to save time, cost and effort. Several procedures have been developed to be used as standard methods for the analysis of sulfonylureas [3–6]. However, none of these methods were suitable for routine analysis. Some of them used solvent extrac-

* Corresponding author.
E-mail address: ggenidy@hotmail.com (G.G. Mohamed).

1386-1425/$ – see front matter © 2009 Elsevier B.V. All rights reserved.
doi:10.1016/j.saa.2009.07.011

tion in sample preparation [4,5] which is a time consuming process and loss of sample may frequently occur during extraction due to emulsion formation in addition to the reported low recovery. Even though Paroni et al. [3] used solid phase extraction (SPE) utilizing OASIS® HLB cartridges, they used five washing steps during the extraction process which is not practical and is time consuming, in addition they used a gradient elution HPLC method. The SPE method developed by Strausbauch et al. [6] was only validated for urine samples. A more important limitation for implementing the previously mentioned procedures for routine analysis of antidiabetic medications is that they were all developed for estimation of glipizide, gliclazide and glibenclamide but not for glimperide or metformin. Until now glimperide was only analyzed in biological matrices by an HPLC method using derivatisation and solvent extraction which is tedious and time consuming [7]. Glimperide is relatively new and it was reported that the commonly used methods for sulfonylurea determination have low sensitivity for glimperide determination [7]. Niemi et al. [8] used an HPLC–mass spectrometry (MS) method for studying the effect of rifampicin on the pharmacokinetics of glimperide, however, the method was not validated and the use of MS has the disadvantage of that it is not available in many laboratories. There is no single published method for the simultaneous determination of both metformin and any of the sulfonylureas in biological fluids. A method for determination of metformin and glipizide or gliclazide [9] and a method for the estimation of metformin and glibenclamide from their combined dosage forms [10] have been described previously for use in studying pharmaceutical preparations but not for analysis in biological fluids. When studying the pharmacokinetics of a new formulation containing a combination of metformin and glibenclamide, Martha et al. [1] used two separate methods one for measuring the concentration of metformin and the other for glibenclamide. In summary, in order to save time and money routine therapeutic monitoring requires the availability of a single method that can be used for the simultaneous determination of antidiabetic medications in plasma. Although, many methods have been reported in the literature for the estimation of metformin, gliclazide, glibenclamide and glipizide individually there is no single method reported for the simultaneous estimation of metformin and sulfonylureas. The reported general procedures for sulfonylurea determination did not include glimperide or metformin. In a previous study [11] the first ion pair solid phase extraction technique was developed for the specific HPLC determination of metformin. In this study that method was optimized for the simultaneous determination of a combination of metformin and sulfonylureas.

However, in this work we prepare chelates of Mn(II), Cr(III), Fe(III), Co(II), Ni(II), Cu(II) and Zn(II) transition metals with GCA drug molecule. The solid chelates are characterized using different physico-chemical methods like elemental analyses (C, H, N, S and metal content), IR, magnetic moment and reflectance spectra, and thermal analysis (TG and DTG). Biological activities of the complexes are studied. The structure of GCA drug is given in Fig. 1.

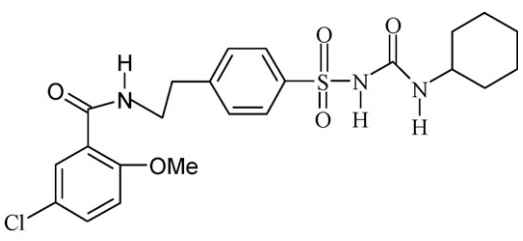

Fig. 1. Structure of GCA drug.

2. Experimental

2.1. Materials and reagents

All chemicals used were of the analytical reagent grade (AR), and of highest purity available. They included glibenclamide (UniPharma); copper(II) chloride dihydrate (Prolabo); cobalt(II) and nickel(II) chlorides hexahydrates (BDH); zinc(II) chloride dihydrate (Ubichem), chromium(III) chloride hexahydrate (Sigma); manganese(II) chloride and ferric(III) chloride hexahydrate (Prolabo). Zinc oxide, disodium salt of ethylenediaminetetraacetic acid; EDTA (Analar), ammonia solution (33%, v/v) and ammonium chloride (El-Nasr Pharm. Chem. Co., Egypt). Organic solvents used included absolute ethyl alcohol, diethylether, and dimethylformamide (DMF). These solvents were spectroscopic pure from BDH and tested for their spectral purity. Hydrogen peroxide, hydrochloric and nitric acids (MERCK) were used. De-ionized water collected from all glass equipments was usually used in all preparations.

2.2. Instruments

The molar conductance of solid complexes in DMF was measured using Sybron–Barnstead conductometer (Meter-PM.6, $E = 3406$). Elemental microanalyses of the separated solid chelates for C, H, N and S were performed in the Microanalytical Center, Cairo University. The analyses were repeated twice to check the accuracy of the data. Infrared spectra were recorded on a PerkinElmer FT-IR type 1650 spectrophotometer in wave number region 4000–400 cm^{-1}. The spectra were recorded as KBr pellets. The solid reflectance spectra were measured on a Shimadzu 3101pc spectrophotometer. The molar magnetic susceptibility was measured on powdered samples using the Faraday method. The diamagnetic corrections were made by Pascal's constant and $Hg[Co(SCN)_4]$ was used as a calibrate. The thermogravimetric (TGA and DrTGA) analysis was carried out in dynamic nitrogen atmosphere (20 mL min^{-1}) with a heating rate of 10 °C min^{-1} using Shimadzu TGA-50H thermal analyzer.

2.3. Synthesis of metal complexes

The metal complexes were prepared by the addition of hot solution (60 °C) of the appropriate metal chloride salts (1 mmol) in an ethanol–water mixture (1:1, 25 mL) to the hot solution (60 °C) of GCA (0.4 g, 1 mmol) in the same solvent (25 mL). The resulting mixture was stirred under reflux for 1 h whereupon the complexes precipitated. They were collected by filtration, washed several times with a 1:1 ethanol:water mixture to get ride the excess GCA or metal salt and then with diethyl ether. The analytical data for C, H, N and S were repeated twice.

2.4. Biological activity

In the present study, the larvae of *Musca domestica* were collected from the permanent colony of insect colony of Entomology Department, Faculty of Science, Cairo University. Insects were reared in the laboratory according to the method of Nassar [12] with some modification.

2.5. Bioassay and statistical analysis

Larval, mortalities were observed during the larval period, while pupal and adult mortalities were calculated based on the successfully emerged individuals from the treated larvae. The developmental rates were also studied. Data obtained were analyzed by the Student's *t*-distribution and refined by Bessel correction [13].

Table 1
Analytical and physical data of glibenclamide metal complexes.

Complex	Colour (% yield)	M.p. (°C)	% Found (Calcd.)					μ_{eff} (B.M.)	Λ_m (Ω^{-1} mol^{-1} cm^2)
			C	H	N	S	M		
$[Cr(H_3L)Cl_3(H_2O)]\cdot 3H_2O$	Red	>300	38.19	4.97	5.56	4.05	8.38		20.46
$C_{23}H_{36}Cl_4CrN_3O_6S$	(70)		(38.10)	(4.73)	(5.80)	(4.42)	(8.76)		
$[Mn(H_3L)Cl_2]\cdot H_2O$	Brown	>300	43.77	4.65	6.80	4.72	8.70	4.70	15.80
$C_{15}H_{23}Cl_2N_3MnO_4S$	(73)		(43.33)	(4.71)	(6.59)	(5.02)	(8.48)		
$[Fe(H_3L)Cl_3(H_2O)]$	Red	>300	40.67	4.13	5.96	4.48	8.10	5.88	25.11
$C_{23}H_{30}Cl_4FeN_3O_6S$	(68)		(40.92)	(4.45)	(6.23)	(4.74)	(8.30)		
$[Co(H_3L)Cl_2(H_2O)_2]$	Red	>300	41.71	5.16	6.52	4.49	9.05	5.66	16.80
$C_{23}H_{32}Cl_3CoN_3O_7S$	(65)		(41.82)	(4.85)	(6.36)	(4.85)	(8.94)		
$[Ni(H_3L)Cl_2(H_2O)_2]\cdot 3H_2O$	Brown	>300	38.46	5.20	6.12	4.62	8.00	3.94	19.74
$C_{23}H_{38}Cl_3NiN_3O_{10}S$	(74)		(38.66)	(5.32)	(5.88)	(4.48)	(8.26)		
$[Cu(H_3L)Cl_2(H_2O)_2]\cdot 2H_2O$	Red	>300	39.15	5.53	5.79	4.34	8.70	1.84	22.07
$C_{23}H_{36}Cl_3CuN_3O_9S$	(76)		(39.40)	(5.14)	(6.00)	(4.57)	(9.06)		
$[Zn(H_3L)Cl_2]$	Red	>300	43.70	3.97	7.02	5.23	10.15	Diam.	16.50
$C_{23}H_{28}Cl_3N_3O_5SZn$	(65)		(43.81)	(4.44)	(6.67)	(5.08)	(10.32)		

3. Results and discussion

The formations of metal complexes with organic compounds have long been recognized. However, the binary complexes of the cited drug with metal ions have not been studied yet, although they may be an area of interest. This is because they may affect the bioavailability of these drugs as certain metal ions were present in relatively appreciable concentration in biological fluids [14].

3.1. Composition and structures of metal complexes

The isolated solid complexes of Cr(III), Mn(II), Fe(III), Co(II), Ni(II), Cu(II) and Zn(II) ions with the GCA drug are subjected to elemental analyses (C, H, N, S and metal content), IR, magnetic moment studies, molar conductance and thermal analysis (TG), to identify their tentative formulae in a trial to elucidate their molecular structures. The results of elemental analyses listed in Table 1 suggest the formulae $[M(H_3L)Cl_n(H_2O)m]\cdot yH_2O$ (where M = Cr(III) ($n=3$, $m=1$, $y=3$); Mn(II) ($n=2$, $m=0$, $y=1$); Fe(III) ($n=3$, $m=1$, $y=0$), Co(II) ($n=2$, $m=2$, $y=0$); Ni(II) ($n=2$, $m=2$, $y=3$); Cu(II) ($n=2$, $m=2$, $y=2$) and Zn(II) ($n=2$, $m=0$, $y=0$).

3.2. Molar conductivity measurements

The chelates are dissolved in DMF and the molar conductivities of 10^{-3} M of their solutions at 25 °C are measured. Table 1 shows the molar conductance values of the complexes. It is concluded from the results that the chelates are found to have molar conductance values of 15.80–25.11 Ω^{-1} mol^{-1} cm^2 indicating that all the metal chelates are none electrolytes.

3.3. IR spectral studies

The IR data of the spectra of GCA ligand and its complexes are listed in Table 2. The IR spectra of the complexes are compared with those of the free GCA ligand in order to determine the coordination sites that may be involved in chelation. The tautomeric equilibrium depends on the extent of conjugation, nature and position of the substituents, polarity of the solvent, etc. This phenomenon has drawn considerable attention by several investigators and characteristic spectral bands have been assigned to the individual tautomers.

The sharp band at 1644 cm^{-1} can be assigned to the amide carbonyl of the saturated side chain moiety. A broad band spreading over the region 3025–3120 cm^{-1} can be ascribed to NH groups. Some authors have reported that the amide carbonyl group present in the saturated side chain moiety enolizes. However, the strong α-effect on the saturated side chain moiety prevents the enolization of this carbonyl group. The complexes under investigation have a band near 3100–3000 cm^{-1}, which is due to the N–H stretching of the saturated side chain moiety which supports the presence of the amide NH in the keto form (ii) and not in the enol form (iii) [15]. This band is masked with a very broad band in the region 3500–3000 cm^{-1} in the spectra of the complexes under investigation which may be due to the intermolecular hydrogen bonding in the solid state.

The stretching vibration band; ν(NH), of the sulfonamide group in the free ligand is hidden under the peak of water molecules or due to the enolization. The presence of coordinated water molecules renders it difficult to confirm the enolization of the sulfonamide group. The SO_2 group modes of the GCA drug appear as sharp bands at 1380 and 1105 cm^{-1} due to $\nu_{asym}(SO_2)$ and $\nu_{sym}(SO_2)$, respectively. In the complexes, the asymmetric and symmetric modes are shifted to 1401–1412 and 1125–1162 cm^{-1}, respectively, upon coordination to the metal ions [16,17]. The shift of the SO_2 stretching vibration to higher frequencies may be attributed to the transformation of the sulfonamide (SO_2NH) to give the enol form (SO(OH)N) (Scheme 1, form (ii)) as a result of complex formation to give more stable six-membered ring [16–18]. The IR bands at 815–855 and 752–770 cm^{-1}, $\nu(H_2O)$ of coordinated water, is an indication of the binding of the water molecules to the metal ions. New bands are found in the spectra of the complexes in the regions 552–537 and 425–500 cm^{-1}, which are assigned

Table 2
IR spectra (4000–400 cm^{-1}) of the GCA ligand and its metal complexes.

Compound	ν(OH) enolic	ν(NH)	ν(SO_2) asym.	ν(SO_2) sym.	ν(C=O) amide	ν(M–O)	ν(M–O)
GCA; H_3L	3150–3350 br	3000–3100 br	1380 sh	1105 sh	1644 sh	–	–
$[Cr(H_3L)Cl_3(H_2O)]\cdot 3H_2O$	3150–3362 br	3025 br	1404 sh	1125 m	1619 sh	546 m	494 s
$[Mn(H_3L)Cl_2]\cdot H_2O$	3115–3360 br	3030 br	1401 m	1162 sh	1620 sh	546 m	457 s
$[Fe(H_3L)Cl_3(H_2O)]$	3100–3550 br	3035 br	1403 m	1162 sh	1619 sh	546 m	458 s
$[Co(H_3L)Cl_2(H_2O)_2]$	3180–3550 br	3119 br	1412 m	1158 sh	1618 sh	541 m	440 m
$[Ni(H_3L)Cl_2(H_2O)_2]\cdot 3H_2O$	3190–3370 br	3050 br	1406 m	1161 sh	1650 sh	543 m	459 s
$[Cu(H_3L)Cl_2(H_2O)_2]\cdot 2H_2O$	3200–3450 br	3120 br	1402 m	1125 m	1619 sh	547 m	455 s
$[Zn(H_3L)Cl_2]$	3200–3450 br	3115 br	1402 m	1161 sh	1619 sh	545 m	461 s

sh, sharp; m, medium; s, small; w, weak; br, broad.

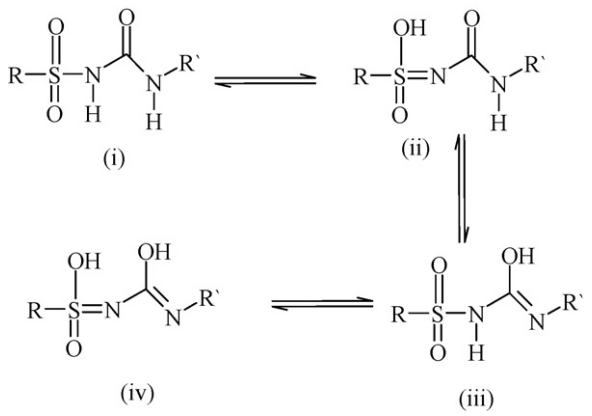

Scheme 1. Tautomeric forms of GCA drug.

to ν(M–O) stretching vibrations of the amide and sulfonamide O atoms [16,17].

Therefore, GCA drug behaves as a neutral bidentate ligand coordinating to the metal ions via amide-*O* and enolic sulphonamide-*OH*.

3.4. Magnetic susceptibility and electronic spectral studies

From the diffuse reflectance spectrum it is observed that, the Fe(III) chelate exhibits a band at 21,470 cm^{-1}, which can be attributed to the $^6A_{1g} \rightarrow T_{2g}(G)$ transition in octahedral geometry of the complexes [19,20]. The $^6A_{1g} \rightarrow {}^5T_{1g}$ transition is found to split into two bands at 17,740 and 15,498 cm^{-1}. The observed magnetic moment of Fe(III) complex is 5.88 B.M. Thus, the complex formed has the octahedral geometry [19,20]. The spectrum shows also a band at 27,690 cm^{-1} which may attributed to ligand to metal charge transfer. The diffuse reflectance spectrum of the Mn(II) complex shows three bands at 16,445, 22,965 and 27,265 cm^{-1}. These bands can be assigned to $^6A_{1g} \rightarrow {}^4T_{1g}$, $^6A_{1g} \rightarrow {}^4T_{2g}(G)$ and $^6A_{1g} \rightarrow {}^4T_{2g}(D)$ transitions, respectively [20]. The room temperature magnetic moment value is found to be 4.70 B.M., which indicates the presence of Mn(II) complex in tetrahedral structure.

The electronic spectrum of the Co(II) complex with the general formula $[Co(H_3L)Cl_2(H_2O)_2]$ gives three bands at 16,946, 18,674 and 22,025 cm^{-1}. The bands observed are assigned to the transitions $^4T_{1g}(F) \rightarrow {}^4T_{2g}(F)$ (ν_1), $^4T_{1g}(F) \rightarrow {}^4A_{2g}(F)$ (ν_2) and $^4T_{1g}(F) \rightarrow {}^4T_{2g}(P)$ (ν_3), respectively, suggesting an octahedral geometry around Co(II) ion [20,21]. The complex is found to have magnetic susceptibility value of 5.66 B.M. (Table 1), indicating an octahedral geometry. The region at 24,660 cm^{-1} refers to the charge transfer band.

The Ni(II) complex; $[Ni(L)_2(H_2O)_2]Cl_2{\cdot}4H_2O$, has a room temperature magnetic moment value of 3.94 B.M.; which is in the normal range observed for octahedral Ni(II) complexes [20–22]. The electronic spectrum displays three bands in the solid reflectance spectrum at ν_1: 16,470 cm^{-1}: $^3A_{2g} \rightarrow {}^3T_{2g}$; ν_2: 18,455 cm^{-1}: $^3A_{2g} \rightarrow {}^3T_{1g}(F)$ and ν_3: 21,562 cm^{-1}: $^3A_{2g} \rightarrow {}^3T_{1g}(P)$. The spectrum shows also a band at 24,665 cm^{-1} which may attributed to ligand to metal charge transfer.

The μ_{eff} value of the Cu(II) complex is 1.84 B.M. indicative of square planar geometry. In confirmation of this structure only one band is seen in the spectrum around 13,889 with two shoulders on either side at 18,868 and 11,905 cm^{-1}. These are assigned to $^2B_{1g} \rightarrow {}^2A_{1g}$, $^2B_{1g} \rightarrow {}^2B_{2g}$ and $^2B_{1g} \rightarrow {}^2E_{2g}$ transitions, respectively [20,23].

The Zn(II) complex is diamagnetic and tetrahedral geometry is proposed for this complex.

3.5. Thermal analyses (TG and DTG)

In the present investigation, heating rates are suitably controlled at 10 °C min^{-1} under nitrogen atmosphere and the weight loss is measured from the ambient temperature up to ≅1000 °C. The data are listed in Table 3. The weight losses for each chelate are calculated within the corresponding temperature ranges. The different thermodynamic parameters are listed in Table 4.

$[Cr(H_3L)Cl_3(H_2O)]{\cdot}3H_2O$ and $[Ni(H_3L)Cl_2(H_2O)_2]{\cdot}3H_2O$ complexes are thermally decomposed in six decomposition steps, within the temperature range of 30–1000 °C. The first decomposition step with an estimated mass loss of 7.77% (calcd. 7.45%) and 5.34% (calcd. 5.04%) within the temperature range 30–120 and 30–100 °C for Cr(III) and Ni(II) complexes, respectively, may be attributed to the liberation of the water molecules of hydration. The remaining decomposition steps found within the temperature range from 120–1000 and 100–1000 °C with an estimated mass losses of 82.17% (calcd. = 81.91%) and 84.47% (calcd. 84.46%) for Cr(III) and Ni(II) complexes, respectively, which are reasonably

Table 3
Thermal analyses (TGA and DTA) data GCA drug and its metal complexes.

Compound	TG range (°C)	$DrTGA_{max}$ (°C)	n^a	%Found (calcd..)		Assignment	Metallic residue
				Mass loss	Total mass loss		
$[Cr(H_3L)Cl_3(H_2O)]{\cdot}3H_2O$	30–120	80	1	7.77 (7.45)		Loss of $3H_2O$	$(1/2)Cr_2O_3$
	120–220	191	1	12.45 (12.28)		Loss of H_2O and Cl_2	
	220–1000	253, 338, 620, 780	4	69.82 (69.63)	90.04 (89.36)	Loss of HCl and remaining ligand	
$[Mn(H_3L)Cl_2]{\cdot}H_2O$	30–110	75	1	2.43 (2.83)		Loss of H_2O	MnO
	110–1000	242, 364, 530, 910	4	86.18 (86.19)	88.61 (89.02)	Loss of Cl_2 and ligand	
$[Fe(H_3L)Cl_3(H_2O)]$	180–230	208	1	5.70 (5.41)		Loss of HCl	$(1/2)Fe_2O_3$
	230–1000	338, 375, 625	3	79.47 (79.66)	85.17 (85.07)	Loss of Cl_2 and $2H_2O$ and remaining ligand	
$[Co(H_3L)Cl_2(H_2O)_2]$	100–230	197	1	21.06 (21.11)		Loss of CH_3OH, Cl_2 and $2H_2O$	CoO
	230–900	402, 650	2	67.41 (67.58)	88.47 (88.69)	Loss of remaining ligand.	
$[Ni(H_3L)Cl_2(H_2O)_2]{\cdot}3H_2O$	30–100	50	1	5.34 (5.04)		Loss of $2H_2O$.	NiO
	100–250	204	1	17.57 (17.51)		Loss of $3H_2O$ and Cl_2	
	250–1000	270, 354, 608, 820	4	66.90 (66.95)	89.81 (89.50)	Loss of remaining ligand	
$[Cu(H_3L)Cl_2(H_2O)_2]{\cdot}2H_2O$	50–230	155	1	10.71 (10.28)		Loss of $4H_2O$	CuO
	230–300	264	1	10.06 (10.14)		Loss of Cl_2	
	300–1000	342, 820	2	67.72 (68.24)	88.49 (88.66)	Loss of remaining ligand	
$[Zn(H_3L)Cl_2]$	120–260	227	1	11.85 (11.27)		Loss of Cl_2	ZnO
	260–1000	351, 820	2	75.59 (75.87)	87.44 (87.14)	Loss of remaining ligand	

[a] *n*, number of decomposition steps.

Table 4
Thermodynamic data of the thermal decomposition of GCA metal complexes.

Complex	Decomp. temp. (°C)	E^* kJ mol^{-1}	A s^{-1}	ΔS^* JK^{-1} mol^{-1}	ΔH^* kJ mol^{-1}	ΔG^* kJ mol^{-1}
$[Cr(H_3L)Cl_3(H_2O)]\cdot 3H_2O$	30–120	34.95	1.77×10^9	−30.55	45.68	68.17
	120–220	63.54	2.39×10^{13}	−75.86	99.26	103.2
	220–420	109.4	4.22×10^{12}	−130.4	168.4	182.4
	420–600	182.6	5.19×10^7	−185.1	206.1	235.9
	600–800	245.4	3.58×10^8	−220.3	230.4	255.2
	800–1000	278.2	5.68×10^9	−242.5	266.5	282.6
$[Mn(H_3L)Cl_2]\cdot H_2O$	30–110	23.95	2.47×10^7	−34.95	45.15	57.22
	110–250	82.44	5.45×10^{11}	−79.16	97.86	106.2
	250–410	142.1	6.28×10^8	−140.2	175.2	199.5
	410–680	176.2	1.46×10^9	−203.1	235.1	262.1
	680–1000	220.3	6.21×10^7	−253.9	280.7	302.1
$[Fe(H_3L)Cl_3(H_2O)]$	180–230	59.28	2.93×10^9	−44.89	60.12	78.96
	230–480	97.46	4.28×10^{11}	−89.55	95.69	110.0
	480–720	144.2	3.95×10^{12}	−156.5	178.9	195.2
	720–1000	205.7	6.23×10^{10}	−197.5	207.4	229.1
$[Co(H_3L)Cl_2(H_2O)_2]$	100–230	62.95	2.99×10^{10}	−53.18	65.78	88.23
	230–520	105.3	4.48×10^8	−108.2	116.4	138.9
	520–900	167.4	5.64×10^{13}	−172.4	196.8	216.5
$[Ni(H_3L)Cl_2(H_2O)_2]\cdot 3H_2O$	30–100	50.55	1.03×10^{13}	−40.44	50.18	78.26
	100–250	102.9	3.70×10^8	−89.27	106.2	130.3
	250–430	157.8	5.62×10^9	−132.4	156.1	182.4
	430–650	190.2	3.42×10^{10}	−188.9	225.4	243.2
	650–810	242.1	5.12×10^{11}	−240.6	260.9	275.4
	810–1000	260.9	4.09×10^9	−306.2	334.2	360.1
$[Cu(H_3L)Cl_2(H_2O)_2]\cdot 2H_2O$	50–230	44.58	3.15×10^8	−45.14	60.56	72.40
	230–300	82.65	4.69×10^7	−98.28	109.6	120.4
	300–660	130.7	6.06×10^{12}	−160.7	198.2	242.1
	660–1000	193.4	4.81×10^{10}	−233.2	275.1	299.2
$[Zn(H_3L)Cl_2]$	120–260	52.78	1.85×10^9	−52.94	72.36	92.44
	260–530	102.3	2.99×10^{12}	−105.2	119.8	138.4
	530–1000	162.4	4.06×10^{12}	−186.7	208.2	252.4

accounted for the removal of H_2O and Cl_2, HCl and remaining ligand as gases.

The thermogram of $[Fe(H_3L)Cl_3(H_2O)]$ chelate shows four decomposition steps within the temperature range from 180–1000 °C. The first step of decomposition within the temperature range from 180 to 230 °C corresponds to the loss of HCl gas with a mass loss of 5.70% (calcd. 5.41%). The energy of activation is found to be 59.28 kJ mol^{-1}. The subsequent steps (230–1000 °C) correspond to the removal of Cl_2 and $2H_2O$ and remaining ligand leaving metal oxide as a residue. The overall weight loss amounts to 85.17% (calcd. 85.07%).

The TG curves of the Co(II) and Zn(II)-chelates show three stages of decomposition within the temperature range of 100–900 and 120–1000 °C, respectively. The stage at 100–230 or 120–260 °C corresponds to the loss of CH_3OH, Cl_2 and $2H_2O$ or Cl_2 for Co(II) and Zn(II) complexes, respectively. The energy of activation for this step is 62.95 and 52.78 kJ mol^{-1} for Co(II) and Zn(II) complexes, respectively. While the subsequent stages involve the loss of ligand molecules with a mass loss of 67.41% (calcd. 67.58%) and 75.59% (calcd. 75.87%) for Co(II) and Zn(II) complexes, respectively. The overall weight loss amounts to 88.47% (calcd. 88.69%) and 87.44% (calcd. 87.14%) for Co(II) and Zn(II) chelates, respectively.

On the other hand $[Mn(H_3L)Cl_2]\cdot H_2O$ chelate exhibits five decomposition steps. The first step within the temperature range from 30–110 °C (mass loss = 2.43%; calcd. for H_2O; 2.83%) may accounted for the loss of one water molecule of hydration. The energy of activation for this step is 23.95 kJ mol^{-1}. As shown in Table 3, the mass losses of the remaining decomposition steps amount to 86.18% (calcd. 86.19%). They correspond to the removal of Cl_2 and remaining ligand molecules leaving MnO as a residue. The energy of activation for these steps is 82.44–20.3 kJ mol^{-1} for the remaining steps.

The TG curves of the Cu(II) chelate represents four decomposition steps as shown in Table 3. The first two steps of decomposition within the temperature range of 50–300 °C correspond to the loss of hydrated water molecules and Cl_2 with a mass loss of 20.77% (calcd. 20.42%). The remaining steps of decomposition within the temperature range 300–1000 °C correspond to the removal of ligand as gases with activation energy of 130.7–193.4 kJ mol^{-1} for the third and fourth steps. The overall weight loss amounts to 88.49% (calcd. 88.66%).

3.6. Kinetic data

The thermodynamic activation parameters of decomposition processes of dehydrated complexes namely activation energy (E^*), enthalpy (ΔH^*), entropy (ΔS^*) and Gibbs free energy change of the decomposition (ΔG^*) are evaluated graphically by employing the Coats–Redfern relation [24]. The entropy of activation (ΔS^*), enthalpy of activation (ΔH^*) and the free energy change of activation (ΔG^*) are calculated using the following equations:

$$\Delta S* = 2.303\,[\log(Ah/kT)]R \quad (1)$$

$$\Delta H* = E* - RT \quad (2)$$

$$\Delta G* = \Delta H* - T\Delta S* \quad (3)$$

The data are summarized in Table 4. The activation energies of decomposition are found to be in the range 32.95–263.6 kJ mol^{-1}. The high values of the activation energies reflect the thermal stability of the complexes. The entropy of activation is found to have negative values in all the complexes which indicate that the decomposition reactions proceed with a lower rate than the normal ones.

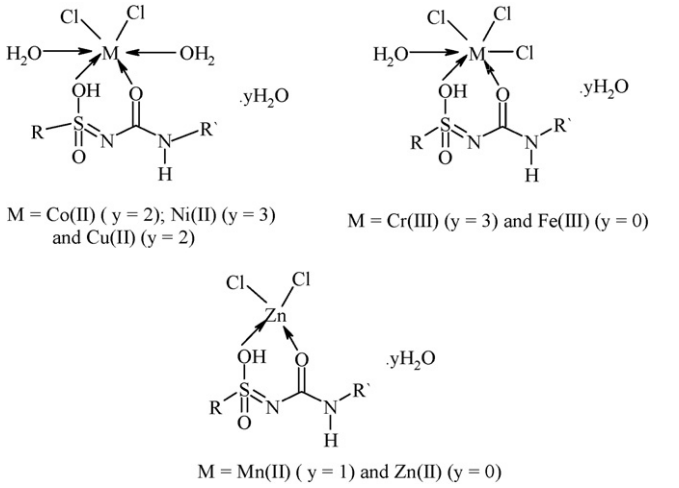

Fig. 2. Proposed structures of GCA metal complexes.

3.7. Structural interpretation

The structures of the complexes of GCA drug with Cr(III), Mn(II), Fe(III), Co(II), Ni(II), Cu(II) and Zn(II) ions are confirmed by the elemental analyses, IR, molar conductance, magnetic, solid reflectance, and thermal analysis (TG) data. Therefore, from the IR spectra, it is concluded that GCA drug behaves as a neutral bidentate ligand coordinated to the metal ions via the enolic sulphonamide-*OH* and amide-*O*. The molar conductance data, it is found that the complexes are non-electrolytes. On the basis of the above observations and from the magnetic and solid reflectance measurements, octahedral and tetrahedral geometries are suggested for the investigated complexes. As a general conclusion, the structures of the metal complexes can be given as shown below (Fig. 2).

3.8. Biological activity

The activities of all the tested complexes may be explained on the basis of chelation theory; chelation reduces the polarity of the metal atom mainly because of partial sharing of its positive charge with the donor groups and possible π electron delocalization within the whole chelate ring. Also, chelation increases the lipophilic nature of the central atom which subsequently favors its permeation through the lipid layer of the cell membrane [25].

In testing the biological activity of GCA drug and its metal complexes, we used larvae of *M. domestica* to increase the chance of detecting antibiotic principles in tested materials.

3.9. Lethal effects

In focusing to the data recorded in Table 5, it appears the potential effects of the different compounds of GCA and its complexes against the treated larvae of *M. domestica*. Larval mortality is found to be 40% due to the effect of Fe(III) and Cu(II) complexes. While the Ni(II) and Zn(II) complexes causes 80 and 70% of the pupal mortality. The higher adult mortality is found to be 60% followed by 50% by the effect of GCA drug and its Cr(III) complex, respectively, in comparison to 0.0% mortality of control insect (Table 5).

Table 5
Effect of Leufenuron and Diofenolan on the larvae, pupae and adults mortalities of the red palm weevil *Rhynchophorus ferrugineus*.

Chemical compounds	Larval mortality	Pupal mortality	Adult mortality
H_3L	–	40	60
$[Cr(H_3L)Cl_3(H_2O)]\cdot 3H_2O$	10	40	50
$[Fe(H_3L)Cl_3(H_2O)]$	40	30	30
$[Ni(H_3L)Cl_2(H_2O)_2]\cdot 3H_2O$	10	80	40
$[Cu(H_3L)Cl_2(H_2O)_2]\cdot 2H_2O$	40	30	30
$[Zn(H_3L)Cl_2]$	10	70	20
Control	–	–	–

3.10. Morphogenic effects

Topical application of GCA drug and its complexes on the different developmental stages of *M. domestica* resulted in different morphogenic abnormalities of pupation and adult emergence. On the other hand, the pupation program is impaired in different degrees by the various compounds. This effect is approximately a compound-dependent. Contrary, the GCA drug has no effect on the larval mortality. On the other hand the larval, pupal and adult deformations are increased by the effect of Cr(III), Ni(II) and Zn(II) complexes. The majority of the observed morphogenic effects represented as shrinking of skin with black colour and larval–pupal intermediate.

The toxicity effect of GCA drug seems to be due to the penetration of the different chemical compounds is inversely proportional to the thickness of the insect cuticle. These results are in good agreement with those previously published [26–28]. It is clear from the data obtained that the larval instar was more tolerant to the chemical compounds than the pupal and adult stages. This can be attributed to insect size [29]. On the other hand toxicity effects of GCA drug and its complexes can be attributed also to the decrease of blood glucose level in insect [30]. Sulphonylurea drugs such as GCA were found to inhibit fluid secretion and metabolism of *Drosophila melanogaster* fly [31]. The insecticidal efficacy on 3rd larval instar and adult fecundity of *M. domestica* was due to metabolism disturbance by the effect of *Trigonella foenum* extracts [32]. In comparison, the variable effects of GCA on the different developmental stages of *M. domestica* are found to be strengthens resistance for some complexes.

The complexes that were found to produce morphological abnormalities can be attributed to their effects on total protein content which inhibited the cholinesterase, esterase enzymes and alkaline acid phosphatases in the blood of the different stages of *M. domestica* [33]. Topical application of the GCA complexes on the larval instars of the *M. domestica*, in the present study, resulted in pronouncedly prohibition of the pupation and adult emergence. It may be considered as a result either to the haemolymph ecdysteroids. In other words, GCA complexes are classified in the category of chitin inhibitors. Morphological abnormalities due to its effect on total protein content which inhibited the cholinesterase, esterase enzymes and alkaline acid phosphatases in the blood of the different stages of *M. domestica* [33].

To clarify the possible morphogenic action of GLZ on the larvae, pupae and adult eclosion programmes, available data in the present study unambiguously prevailed increased deformity, approximately, by the decreasing dose-level of *M. domestica* [34], *Musa stabulans* [33,34] and *Rhynchophorus ferrugineus* [35,27].

References

[1] P. Martha, M. Arnold, J. Meeker, D. Greene, J. Clin. Pharmacol. 40 (2000) 1494.
[2] C. Tack, P. Smits, The Netherland J. Med. 55 (1999) 209.
[3] R. Paroni, B. Comuzzi, C. Arcelloni, S. Brocco, Clin. Chem. 64 (2000) 1773.
[4] S. Sved, I. McGilveray, N. Beaudoin, J. Pharm. Sci. 65 (1976) 1356.
[5] A. Sener, A. Akkan, W. Malaisse, Acta Diabetol. 32 (1995) 64.
[6] M. Strausbauch, S. Xu, J. Ferguson, M. Nunez, J. Landers, J. Chromatogr. A 717 (1995) 279.
[7] K. Lehr, P. Damm, J. Chromatogr. 526 (1990) 479.
[8] M. Niemi, K. Kivisto, T. Backman, J. Clin. Pharmacol. 50 (2000) 591.
[9] M. Vasudevan, J. Ravi, B. Suresh, J. Pharm. Biomed. Anal. 25 (2001) 77.
[10] D. Khanolkar, V. Shinde, Indian Drugs 36 (1999) 739.
[11] S. AbuRuz, J. Millership, J. McElnay, J. Chromatogr. B 798 (2003) 203.

[12] M.M.I. Nassar. Some biological and toxicologica studies on the false stable fly, *Muscina stabulans* (Fallen) (Diptera—Muscidae), MS Thesis, Entomol. Dept. Fac. of Sci., Cairo Univ., 1988.
[13] M.J. Moroney, Facts From Figures, 3rd ed., Penguin Books Ltd., Harmonds Worth Middlesex, 1956.
[14] F. Salama, N. El-Abasawy, S.A. Abdel Razeq, M.M.F. Ismail, M.M. Fouad, J. Pharm. Biomed. Anal. 33 (2003) 411.
[15] (a) H.C. Yao, P. Resnick, J. Am. Chem. Soc. 84 (1962) 3514;
(b) F. Kaberia, B. Vickery, G.R. Willey, Drew MGB, J. Chem. Soc., Perkin Trans. 2 (1980) 1622.
[16] G. Gehad, C.M. Mohamed, Sharaby, Spectrochim. Acta Part A 66 (2007) 949.
[17] N. Raman, A. Kulandaisamy, K. Jeyasubramanian, Synth. React. Inorg. Met. Org. Chem. 31 (7) (2001) 1249.
[18] S.D. Kolwalkar, B.H. Mehta, Asian J. Chem. 8 (1996) 406.
[19] M.A. Zayed, F.A. Nour El-Dien, G. Gehad, Mohamed, E.A. Nadia, El-Gamel, J. Mol. Struct. 841 (1–3) (2007) 41–50.
[20] F.A. Cotton, G. Wilkinson, C.A. Murillo, M. Bochmann, Advanced Inorganic Chemistry, 6th ed., Wiley, New York, 1999.
[21] G. Gehad, Mohamed, A. Nasser, Ibrahim, A.E. Hanaa, Attia, Spectrochim. Acta Part A 72 (2009) 610.
[22] G. Gehad, Mohamed, Phosphorus, Sulfur, Silicon Relat. Elements 180 (2005) 1569.
[23] P.R. Shukla, V.K. Singh, A.M. Jaiswal, G. Narain, J. Ind. Chem. Soc., LX (1983) 321–324.
[24] A.W. Coats, J.P. Redfern, Nature 20 (1964) 68.
[25] A. Caudhary, R.V. Singh, Phosphorous Sulfur Silicon 178 (2003) 603.
[26] E. Bruck, J. Entomol. Germ. 2 (1979) 320.
[27] M.M.I. Nassar, K.S. Ghoneim, A.S. Bream, M.A. Tanani, Inhibitory and toxicity effects of two IGRs (CGA-184699) and (CGA-59205) on the red palm weevil, *Rhynchophorus ferrugineus* (Coleoptera: Curculionidae), in: Proceeding of 4th Conference of Applied Entomology, Cairo Univ., 2008, pp. 82–94.
[28] J.K. Samarasekera, B.P. Khambay, K.P. Hemalal, J. Nat. Prod. Res. 18 (2004) 117.
[29] J.K. Ikeda, R.F.L. Mau, W.C. Mitchell, M. Tamashiro, J. Econ. Entomol. 72 (1979) 33.
[30] M.R. Amin, M. Mostafa, K. Rafi, M.S. Hossain, M.M. Hasan, M.L. Sharmin, J. Biol. Sci. 4 (2004) 323.
[31] J.M. Evan, A.K. Allan, S.A. Davis, J.A.T. Dow, J. Exp. Biol. (2005) 3771.
[32] A.S. Adel Halim, T.A. Morsy, J. Egypt Soc. Parasitol. 36 (2006) 329.
[33] K.S. Ghoneim, N. Essa, R.G. Abul-Ela, A.A. Al-Morsy, M.M.I. Nassar, Al-Azhar, Bull. Sci. 2 (1992) 687.
[34] M.M.I. Nassar. The potential of some juvenoids, precocenes and botanical extracts for the control of *Muscina stabulans* (Falken) (Diptera: Muscidae), Unpublished Ph.D. Thesis, Fac. Sci., Cairo Univ., 1995.
[35] K.S. Ghoneim, A.S. Abdel-Ghaffar, M.A. Bream, M.M.I. Tanani, Nassar, J. Egypt. Acad. Soc. Environ. Develop. A Entomol. 9 (2007) 11.